# REMOVAL OF IMAGE DEFOCUS AND MOTION BLUR EFFECTS WITH A NONLINEAR INTERPOLATIVE VECTOR QUANTIZER

*David G. Sheppard, Kannan Panchapakesan, Ali Bilgin, Bobby R. Hunt, Michael W. Marcellin*

Department of Electrical and Computer Engineering
University of Arizona
Tucson, AZ 85721
sheppard@ece.arizona.edu

## ABSTRACT

In this paper, results are presented which demonstrate removal of image defocus and motion blur effects using an algorithm based on *nonlinear interpolative vector quantization* (NLIVQ). The algorithm is trained on original and diffraction-limited image pairs which are representative of the class of images of interest. The discrete cosine transform is used in the codebook design process to control complexity. Imagery processed with this algorithm demonstrate both qualitative and quantitative improvements (as measured by the peak signal-to-noise-ratio before and after processing).

## I. INTRODUCTION

In the context of image coding, vector Quantization (VQ) is generally considered a data compression technique [1]. However, VQ algorithms have been presented which perform other signal processing tasks concurrently with compression [2]. In earlier work [3, 4, 5], the authors presented a novel algorithm based on *nonlinear interpolative vector quantization* (NLIVQ) [6] intended to address the removal of blur caused by diffraction-limited optics [7, 8]. The results presented in this paper demonstrate the usefulness of the algorithm for removing the effects of image defocus and motion blur.

## II. DESCRIPTION OF THE ALGORITHM

In order to perform image restoration, the algorithm must take as its input a block of pixel data from the blurred input image and estimate the original pixel values. In other words, it must implement a mapping between the two image spaces. The general framework for using VQ in this manner is known as NLIVQ. This section will discuss the algorithm in general terms. For more information, please see references [3, 4, 5].

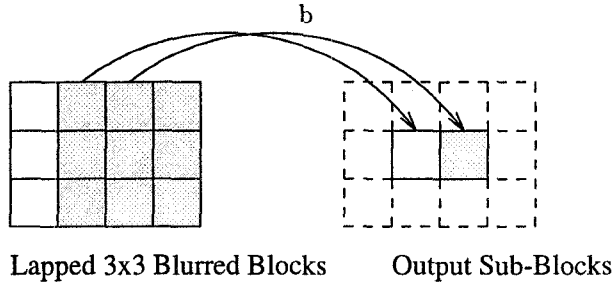


Figure 1: Lapped decoder for 3 × 3 blocks

The algorithm is trained on blocks of pixels drawn from original and degraded image pairs. The imagery in the training set is assumed to be representative of the class of images of interest. Each block is preprocessed using the discrete cosine transform (DCT) in order to manage codebook complexity and avoid costly iterative codebook design. An encoder for the blocks drawn from the degraded images is designed by computing the first and second order statistics of the transform coeeficients, assuming Laplacian distributions for the non-DC coefficients, and proceeding from there to design the minimum mean-squared error encoder for a target bit rate [9]. The one-to-one correspondence between a block drawn from a blurred image and its counterpart in the original induces a decoder based on the original block data. In operation, each block from a degraded image is encoded using the encoder designed above and then decoded using the decoder associated with the original block data. The algorithm used here is the improved version [5] in which image blocks are lapped during decoding, as shown in Fig. 1. This implementation suppresses the blocking artifacts that would otherwise afflict the restored imagery.

This research was supported by the U.S. Air Force Maui Optical Station under contract SC-92C-04-31.

0-7803-4876-1/98/$10.00 © 1998 IEEE

## III. MODELING OF IMAGE DEFOCUS AND MOTION BLUR

The discrete linear, shift-invariant, image formation model [7]

$$g = f * h$$

is assumed, where $g$ is the observed image, $f$ is the original image, $h$ is the point spread function (PSF) of the optical system, and the notation $*$ refers to convolution. The PSF of a defocused incoherent optical system is modeled by computing the aberrated (or generalized) pupil function corrupted with the Zernike polynomial representing image defocus [10]. Given the unaberrated pupil function $P[u,v]$, in pupil coordinates $u,v \in \{-N/2+1, \ldots, N/2\}$, this can be expressed as

$$P_g[u,v] = P[u,v]\exp\{ia\phi[u,v]\},$$

where the parameter $a$ corresponds to the strength of the aberration, and

$$\phi[u,v] = 3.464\rho^2 - 1.732,$$

$$\rho = \frac{\sqrt{u^2+v^2}}{N/2},$$

is the fourth order Zernike polynomial. The PSF is given by

$$h_d[x,y] = \mathcal{F}\{P_g \star P_g\},$$

in image plane coordinates $x,y \in \{-N/2+1, \ldots, N/2\}$, followed by normalization to unit volume [8]. The notation $\star$ refers to correlation. For simplicity, the scaling between the pupil and image plane as a function of wavelength has been ignored.

The effects of motion blur [7] are modeled by assuming a PSF of unit width in the orientation orthogonal to the blur, and n pixels long in the direction of motion. This yields a simple expression for the PSF which is given by

$$h_m[x,y] = 1/n,$$

for $x \in \{-n/2, \ldots, n/2\}$ and $y = 0$, and zero elsewhere.

## IV. SIMULATIONS

These simulation results are obtained by applying the algorithm to mean-removed image blocks. Estimation of the mean of the restored block is dealt with as a separate problem. This allows all of the bits available to be used in representing the non-DC coefficients of each block, resulting in better performance. Restoration of the block mean is done with a Wiener filter process. The parameters for the results below are: 1) $3 \times 3$ blocks; 2) 12 bits/mean-removed block, yielding $R = 2.2$ bits/pixel; 3) a training set of 53 ($512 \times 512$) image pairs of aerial views of urban areas; 4) two defocus and two motion blur OTFs; and 5) varying levels noise in the blurred images. Fig. 2 displays a crop from the "original" test image (outside the training set). This image is similar in content to many of the images in the training set. The remaining figures show the blurred images produced from the original for defocus ($a = 0.9$) and motion blur (horizontal, $n = 7$), and the restorations. For these forms of degradation, the peak signal-to-noise-ratio (PSNR) values of images processed by the algorithm improved substantially. This is summarized in Table 1. The quantitative improvement in the images is matched by significant improvements in visual quality. This is true for images both in and out of the training set. The algorithm clearly functions well in the presence of significant levels of noise.

Figure 2: Sub-image from original test image ($256 \times 256$).

## V. CONCLUSION

Results produced by an algorithm for image restoration based on nonlinear interpolative vector quantiza-

| | Blurred Image Signal-to-Noise Ratio | | | | | | | | | |
|---|---|---|---|---|---|---|---|---|---|---|
| | None | | 30 dB | | 20 dB | | 15 dB | | 10 dB | |
| **Blur Type** | Blur | NLIVQ | Blur | NLIVQ | Blur | NLIVQ | Blur | NLIVQ | Blur | NLIVQ |
| Defocus ($a = 6$) | 24.22 | 28.80 | 24.21 | 28.70 | 24.09 | 27.43 | 23.84 | 25.63 | 23.11 | 22.42 |
| Defocus ($a = 9$) | 22.42 | 28.33 | 22.42 | 27.89 | 22.36 | 25.73 | 22.21 | 23.99 | 21.78 | 21.40 |
| Motion ($n = 5$) | 23.81 | 28.20 | 23.79 | 27.85 | 23.65 | 26.86 | 23.33 | 25.65 | 22.45 | 22.82 |
| Motion ($n = 7$) | 22.74 | 27.49 | 22.73 | 27.02 | 22.63 | 25.79 | 22.42 | 24.57 | 21.77 | 22.07 |

Table 1: Peak signal-to-noise ratio values for images before and after processing.

tion were presented. These demonstrate the utility of the algorithm for images degraded by defocus or motion blur. Both quantitative and qualitative improvements were demonstrated in both cases. The algorithm demonstrated robust performance in the presence of noise.

## VI. REFERENCES


[1] A. Gersho and R. M. Gray, *Vector Quantization and Signal Compression* (Kluwer, MA), 1992.

[2] P. C. Cosman, K. L. Oehler, E. A. Riskin and R. M. Gray, "Using vector quantization for image processing," *Proc. IEEE,* Vol. 81, No. 9, Sep. 1993, 1325–41.

[3] D. G. Sheppard, A. Bilgin, M. S. Nadar, B. R. Hunt, and M. W. Marcellin, "A vector quantizer for image restoration," *Proceedings, 1996 IEEE International Conference on Image Processing,* Lausanne, Switzerland.

[4] D. G. Sheppard, A. Bilgin, M. S. Nadar, B. R. Hunt, and M. W. Marcellin, "A vector quantizer for image restoration," to appear in *IEEE Transactions on Image Processing.*

[5] D. G. Sheppard, K. Panchapakesan, A. Bilgin, B. R. Hunt, and M. W. Marcellin, "Lapped nonlinear interpolative vector quantization and image super-resolution," submitted to *IEEE Transactions on Image Processing.*

[6] A. Gersho, "Optimal nonlinear interpolative vector quantization," *IEEE Trans. Comm.*, Vol. 38, No. 9, Sep. 1990, 1285–87.

[7] H. C. Andrews and B. R. Hunt, *Digital Image Restoration* (Prentice-Hall, NJ), 1977.

[8] J. W. Goodman, *Introduction to Fourier Optics* (McGraw-Hill, NY), 1968.

[9] N. Jayant and P. Noll, *Digital Coding of Waveforms: Principles and Applications to Speech and Video*, (Prentice Hall, NJ), 1980.

[10] M. Born and E. Wolf, *Principles of Optics*, 6th edition, (Pergamon Press, NY), 1980.

Figure 3: Sub-image from defocused image ($a = 0.9$), with SNR = 15 dB ($256 \times 256$).

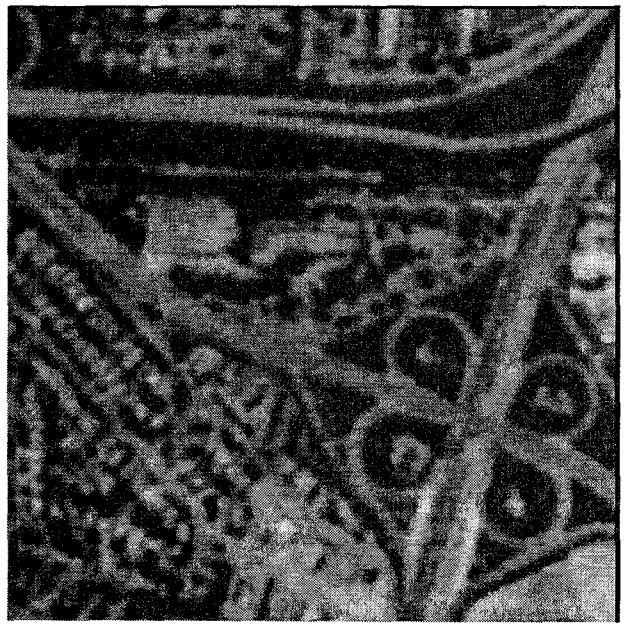

Figure 5: Sub-image from NLIVQ-restoration of defocused image ($a = 0.9$), with SNR = 15 dB ($256 \times 256$).

Figure 4: Sub-image from defocused image ($a = 0.9$), with SNR = 30 dB ($256 \times 256$).

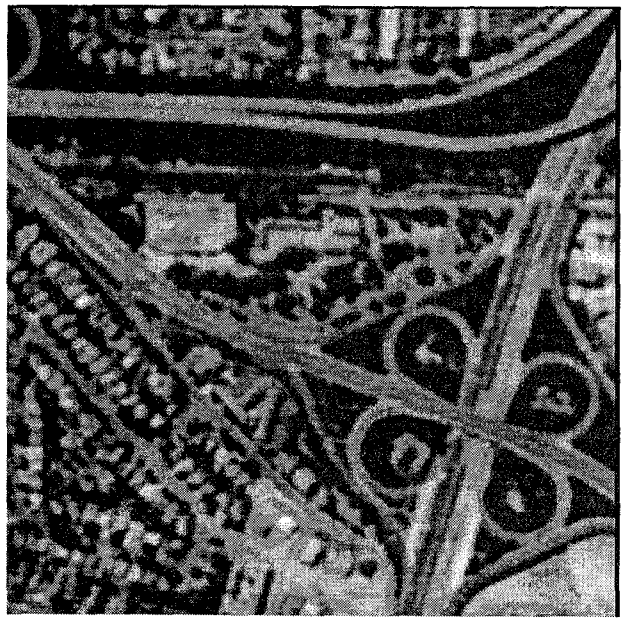

Figure 6: Sub-image from NLIVQ-restoration of defocused image ($a = 0.9$), with SNR = 30 dB ($256 \times 256$).

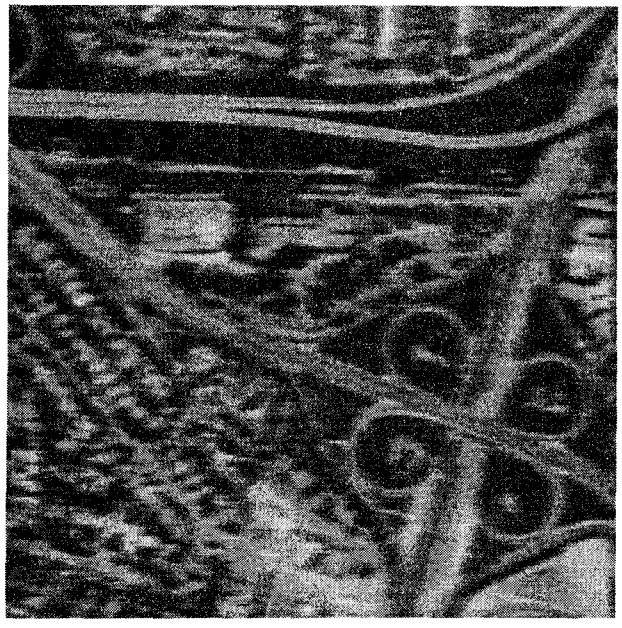

Figure 7: Sub-image from motion-blurred image ($n = 7$), with SNR = 15 dB ($256 \times 256$).

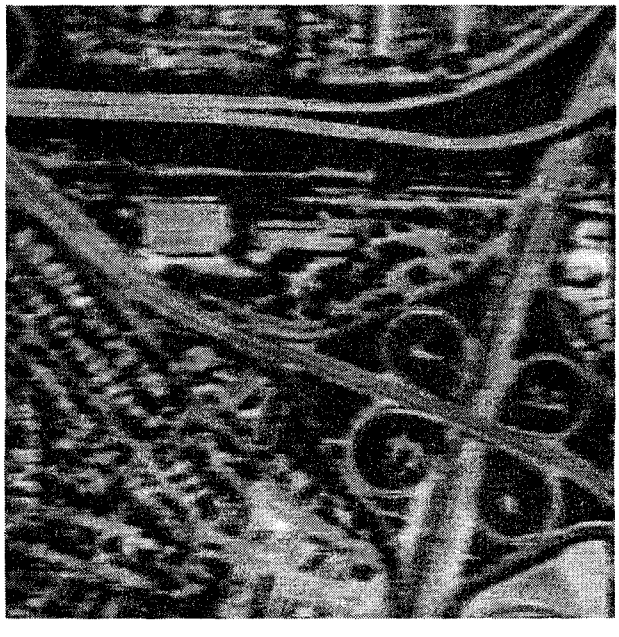

Figure 8: Sub-image from motion-blurred image ($n = 7$), with SNR = 30 dB ($256 \times 256$).

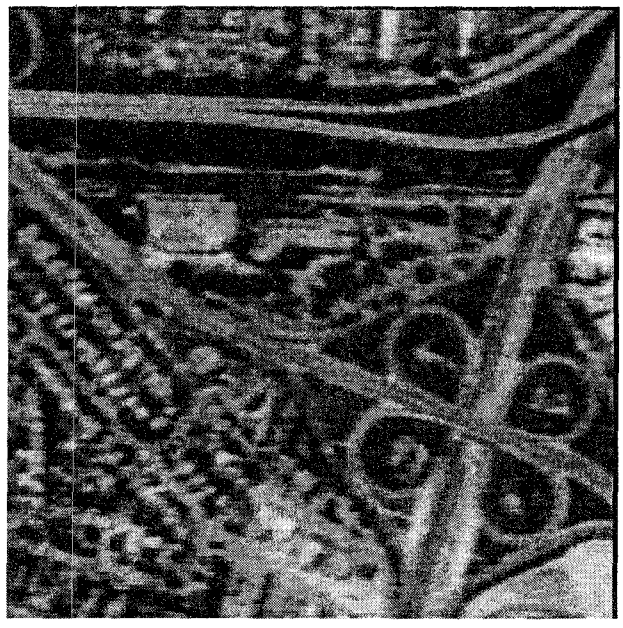

Figure 9: Sub-image from NLIVQ-restoration of motion-blurred image ($n = 7$), with SNR = 15 dB ($256 \times 256$).

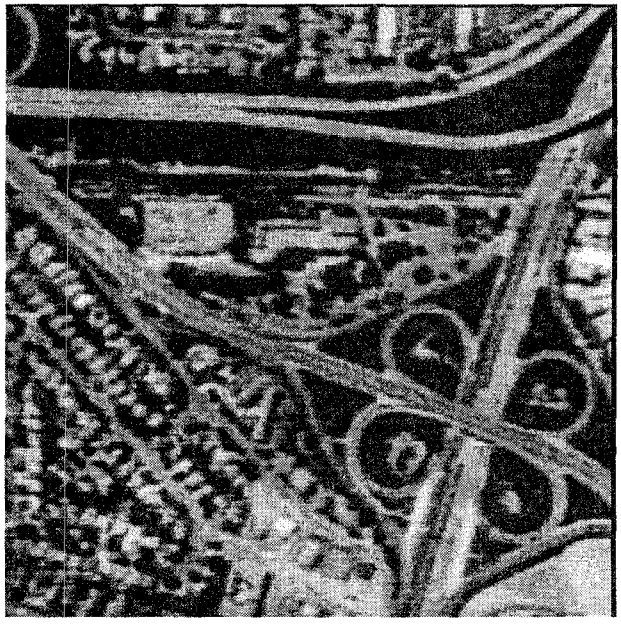

Figure 10: Sub-image from NLIVQ-restoration of motion-blurred image ($n = 7$), with SNR = 30 dB ($256 \times 256$).